

Electronic Supplementary Information

Ion-strength and pH dependent reactivities of ascorbic acid toward ozone in aqueous micro-droplets studied by aerosol optical tweezers

Yuan-Pin Chang,^{a,b,c,1} Shan-Jung Wu,^a Min-Sian Lin,^a Che-Yu Chiang,^a Genin Gy Huang^c

^aDepartment of Chemistry, National Sun Yat-sen University, Kaohsiung 80424, Taiwan

^bAerosol Science Research Center, National Sun Yat-sen University, Sizihwan, Kaohsiung 80424, Taiwan

^cDepartment of Medicinal and Applied Chemistry, Kaohsiung Medical University, Kaohsiung 80708, Taiwan

¹To whom correspondence may be addressed. Email: ypchang@mail.nsysu.edu.tw

I. Experimental conditions

Table S1. Experimental conditions of every reaction kinetic measurements at pH ≈ 2 . P : pressure of gaseous ozone pressure; r : radius; H : Henry's law coefficient; I : ionic strength.

| Expt. # | P / ppm | $[\text{AH}_2]_0$ / M | r / μm | H / mol $\text{m}^{-3} \text{atm}^{-1}$ | I / M | pH | gradient / 10^{-4}s^{-1} | k_2 / 10^5 $\text{M}^{-1} \text{s}^{-1}$ |
|---------|--------------|--------------------------|---------------------|--|---------|-----|---------------------------------------|---|
| 01 | 42 | 3.55 | 3.44 | 4.12 | 1.07 | 1.8 | 13.9 \pm 0.1 | 6.69 \pm 0.82 |
| 02 | 97 | 3.29 | 2.95 | 4.44 | 0.99 | 1.8 | 29.3 \pm 0.2 | 3.30 \pm 0.39 |
| 03 | 110 | 3.82 | 2.71 | 3.81 | 1.15 | 1.8 | 27.2 \pm 0.3 | 2.89 \pm 0.50 |
| 04 | 18.4 | 1.63 | 3.00 | 6.96 | 0.50 | 1.9 | 9.06 \pm 0.29 | 2.13 \pm 0.21 |
| 05 | 18.1 | 2.36 | 2.36 | 5.56 | 0.72 | 1.9 | 9.72 \pm 0.26 | 2.94 \pm 0.31 |
| 06 | 17.6 | 2.77 | 2.45 | 4.90 | 0.85 | 1.8 | 10.3 \pm 0.3 | 5.88 \pm 0.60 |
| 07 | 3.96 | 2.58 | 2.12 | 5.20 | 0.79 | 1.8 | 3.33 \pm 0.12 | 7.45 \pm 0.85 |
| 08 | 2.98 | 3.79 | 2.48 | 3.58 | 1.16 | 1.8 | 2.26 \pm 0.04 | 26.0 \pm 0.3 |
| 09 | 3.12 | 1.79 | 2.12 | 6.61 | 0.55 | 1.9 | 5.17 \pm 0.25 | 12.4 \pm 0.2 |
| 10 | 3.47 | 3.43 | 2.78 | 3.98 | 1.06 | 1.8 | 2.46 \pm 0.02 | 20.8 \pm 0.2 |
| 11 | 3.51 | 2.51 | 1.92 | 5.30 | 0.77 | 1.9 | 4.15 \pm 0.13 | 11.3 \pm 0.1 |
| 12 | 1.88 | 1.96 | 2.10 | 6.31 | 0.59 | 1.9 | 3.52 \pm 0.20 | 18.9 \pm 0.3 |
| 13 | 1.85 | 5.57 | 2.31 | 2.08 | 1.68 | 1.7 | 2.80 \pm 0.06 | 393 \pm 36 |
| 14 | 1.72 | 5.23 | 2.19 | 2.31 | 1.58 | 1.7 | 2.10 \pm 0.04 | 174 \pm 17 |
| 15 | 1.70 | 3.23 | 2.68 | 4.24 | 0.99 | 1.8 | 1.35 \pm 0.02 | 15.7 \pm 1.4 |
| 16 | 1.60 | 3.64 | 2.36 | 3.73 | 1.12 | 1.8 | 1.45 \pm 0.04 | 31.8 \pm 3.1 |
| 17 | 1.13 | 3.13 | 2.79 | 4.39 | 0.95 | 1.8 | 1.28 \pm 0.02 | 39.4 \pm 3.6 |
| 18 | 1.18 | 3.42 | 2.21 | 4.01 | 1.04 | 1.8 | 1.64 \pm 0.04 | 50.2 \pm 5.2 |
| 19 | 1.44 | 3.38 | 2.08 | 4.06 | 1.03 | 1.8 | 1.08 \pm 0.01 | 12.5 \pm 1.3 |

Table S2. Experimental conditions of every reaction kinetic measurements at pH ≈ 6 . P : pressure of gaseous ozone; I : ionic strength; pH_i : pH measured before reaction; pH_f : pH measured after reaction.

| Expt. # | P / ppm | $[\text{AH}_2]_0$ / M | r / μm | H / mol $\text{m}^{-3} \text{atm}^{-1}$ | I / M | pH_i | pH_f | gradient / 10^{-4}s^{-1} | k_2 / 10^7 $\text{M}^{-1}\text{s}^{-1}$ |
|---------|--------------|--------------------------|------------------------|--|------------|---------------|---------------|---------------------------------------|---|
| 20 | 1.17 | 0.98 | 1.90 | 2.17 | 4.25 | 6.3 | 6.5 | 9.07 ± 2.29 | 11.1 ± 4.2 |
| 21 | 0.92 | 0.52 | 2.40 | 4.75 | 2.26 | 6.2 | 6.9 | 8.03 ± 1.71 | 2.48 ± 0.79 |
| 22 | 1.13 | 1.05 | 3.18 | 1.93 | 4.56 | 6.1 | 6.2 | 5.29 ± 0.84 | 15.5 ± 3.8 |
| 23 | 0.90 | 0.89 | 2.34 | 2.53 | 3.86 | 6.3 | 6.4 | 5.15 ± 0.97 | 6.08 ± 1.74 |
| 24 | 0.63 | 0.75 | 2.80 | 2.98 | 3.48 | 6.2 | 6.7 | 4.84 ± 0.42 | 9.54 ± 1.50 |
| 25 | 1.10 | 0.38 | 2.30 | 5.95 | 1.70 | 6.1 | 7.0 | 11.7 ± 0.51 | 1.58 ± 1.00 |
| 26 | 1.07 | 0.85 | 2.20 | 2.63 | 3.81 | 6.4 | 6.5 | 7.18 ± 1.83 | 6.63 ± 2.50 |
| 27 | 1.24 | 0.53 | 2.10 | 4.62 | 2.36 | 6.4 | 6.5 | 10.6 ± 0.35 | 1.97 ± 0.93 |
| 28 | 1.21 | 1.09 | 3.10 | 1.62 | 5.06 | 5.9 | 6.3 | 5.93 ± 1.15 | 23.6 ± 6.9 |
| 29 | 1.19 | 1.14 | 2.70 | 1.48 | 5.30 | 6.4 | 6.8 | 5.01 ± 0.98 | 16.6 ± 4.9 |

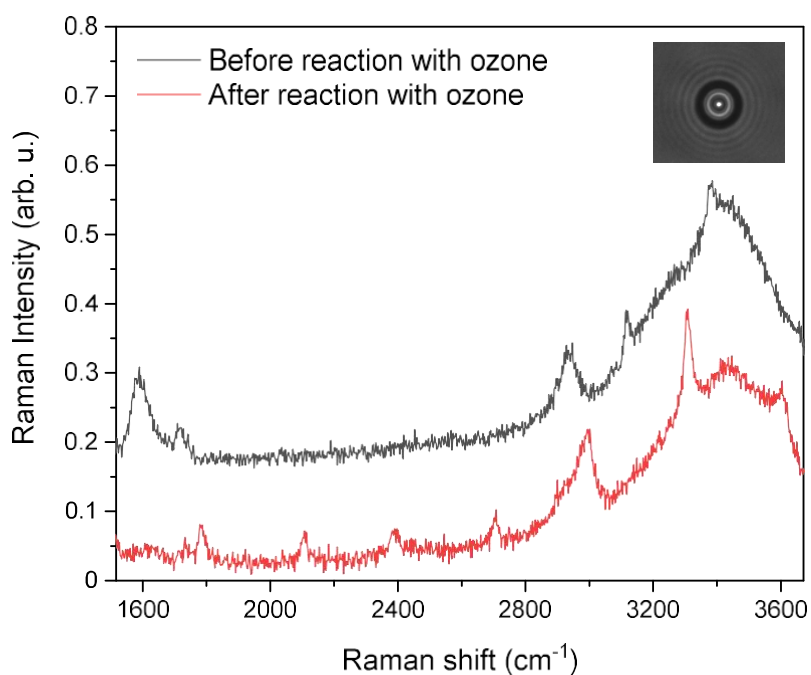


Figure S1. Representative Raman spectra of an optically trapped aqueous AH_2 droplet in $\text{pH} \approx 6$ before (top data in black line) and after (bottom data in red line) the reaction with ozone at 90% RH. Two spectra are offset for clarity. Inset:

brightfield image of the droplet before the reaction with ozone.

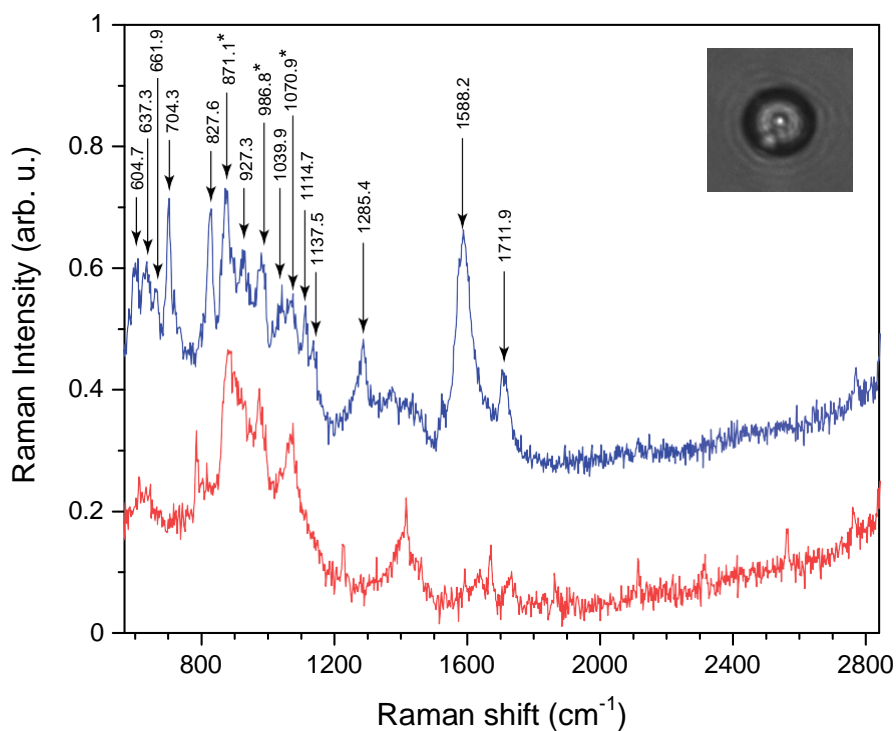


Figure S2. Representative Raman spectra of an optically trapped aqueous AH_2 droplet in $\text{pH} \approx 6$ before (top data in black line) and after (bottom data in red line) the reaction with ozone at 90% RH. Two spectra are offset for clarity. The inset shows the brightfield image of the droplet before the reaction with ozone. The peak assignments (arrows with wavenumbers) without asterisk belong to aqueous AH^- based on literature,¹ and three peak assignments with asterisks belong to phosphate, according to Figure S4. Note that the relatively sharp peaks in the spectra, particularly in the spectrum after the reaction, are CERS peaks.

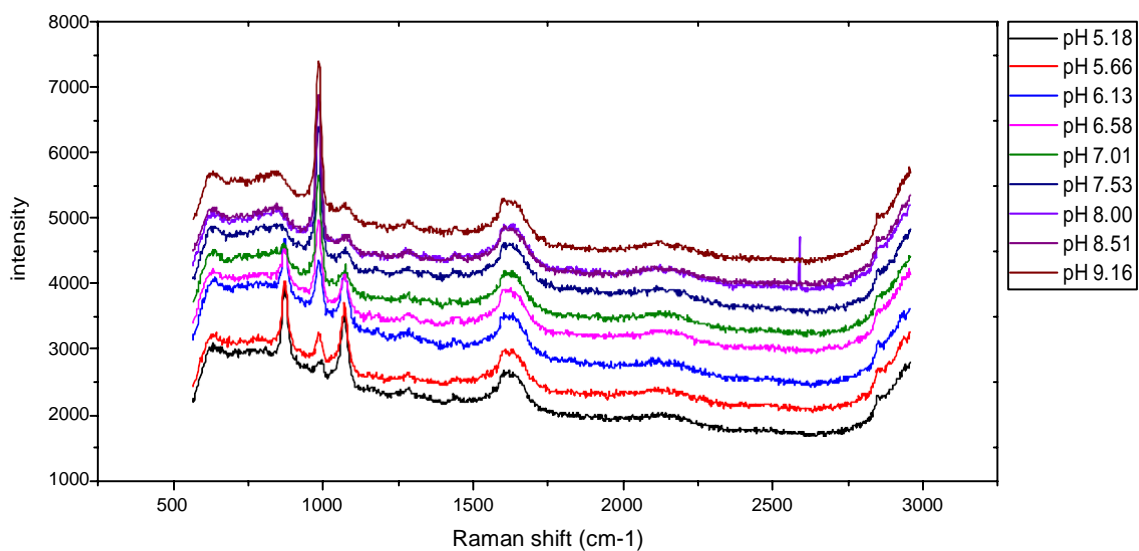


Figure S3. The Raman spectra of 0.5M bulk solutions of sodium phosphate adjusted to specific pH, excited by 532 nm.

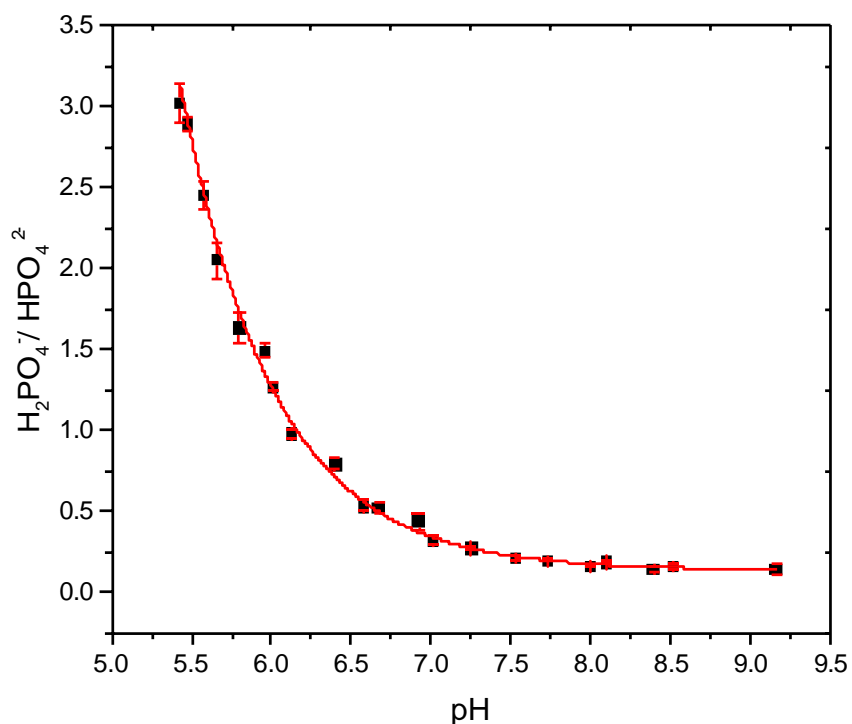


Figure S4. Calibration curve for the pH versus Raman peak area ratios of H_2PO_4^- (874 cm^{-1}) and HPO_4^{2-} (987 cm^{-1}), based on the results in Figure S3. The red curved line is the fit to the data (symbol) which yields the empirical relationship: $y = 0.1338 + 31869 \exp(-x/0.5856)$.

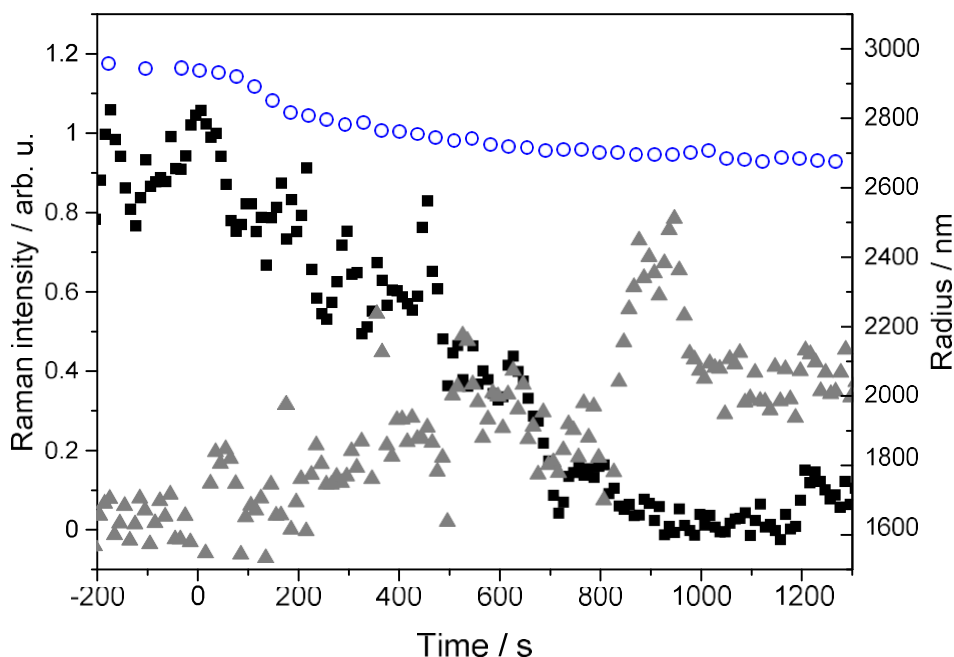


Figure S5. Representative time profiles of radius (circles) and integrated Raman intensities of a trapped $\text{AH}_2(\text{aq})$ droplet of $\text{pH} \approx 6$ (expt. 22) which was exposed to gaseous ozone after 0 second. The Raman intensities of AH_2 (squares) and products (triangles) were obtained from integrating the areas of the Raman peaks centered at 1590 cm^{-1} and 3000 cm^{-1} , respectively. Most jumps in Raman intensities are ascribed to drifting CERS peaks.

II. Effect of ionic strength on Henry's law constant

Here we followed the methodology utilized by Weisenberger and Schumpe² to estimate the Henry's law coefficient of ozone in salt solutions, H_s , with Sechenov constants of ion i , K_i :

$$\log\left(\frac{H}{H_s}\right) = \sum_i K_i [i] = \sum_i (h_i + h_{\text{O}_3}) [i] \quad (\text{S1})$$

where H is the Henry's law coefficient of ozone in pure water, h_i is an ion-specific parameter, h_{O_3} is an ozone-specific parameter, and $[i]$ is the concentration of ion i .

The values of h_i for $i = \text{Na}^+$, Cl^- , HPO_2^- and HPO_4^{2-} have been measured by

Weisenberger and Schumpe.² We cannot find any value of h_i for ascorbate in literature, and thus we assumed its value to be $0.1464 \text{ m}^3/\text{kmol}$, which is the value for IO_4^- , which has the same charge and similar molecular weight of ascorbate. The

expression for the Sechenov constant of ozone, h_{O_3} , is assumed to be a linear function of the temperature T :

$$h_{O_3} = h_{O_3,0} + h_T(T - 298.15K) \quad (S2)$$

with $h_{O_3,0} = 0.00396 \text{ m}^3/\text{kmol}$ and $h_T = 0.00179 \text{ m}^3/(\text{kmol}\cdot\text{K})$.³ The temperature in this study is 298 K. For the case of the aqueous solution containing nonelectrolytes, such as free acid form of AH_2 , the corresponding Sechenov constant K_n can be expressed as:⁴

$$K_n = b_n + b_{O_3,o} + b_{O_3,T}(T - 298.15K) \quad (S3)$$

As we cannot find any literature value of b_n for AH_2 , we assume its value to be $4.81 \times 10^{-4} \text{ m}^3 \text{ kg}^{-1}$, which is the value for citric acid, which has the similar molecular weight of AH_2 .

III. Error analysis

The percentage error of $[AH_2]_0$ is about 4%, which is attributed to fitting error of calibration curves. The error bar of the radius is assumed to be $0.15 \text{ }\mu\text{m}$, which is an averaged change of the radius during the reaction progress. The percentage error of the ozone pressure is 2.6%, which is the assumed maximum error of the measured UV absorption cross section of ozone at 250 nm estimated by literature.⁵ The fitting of each normalized $[AH_2]^{1/2}$ time profile yield an fitting error bar for each fitted gradients listed in Tables S1 and S2. We propagate these error bars through the following equations:

$$\varepsilon^2 = \sum_i \varepsilon_i^2 \quad (S4)$$

where ε is the percentage error of the bimolecular reaction rate coefficient or normalized Raman intensity, and ε_i is the percentage error of each term required to derive the rate coefficient or the normalized Raman intensity. For the function of square root, such as $f = I^{1/2}$, we utilize the following equation to propagate the error of I :

$$\varepsilon_f = \frac{1}{2} \varepsilon_I \quad (S5)$$

where ε_f and ε_I are percentage errors of f and I , respectively.

IV. Droplet size dependence

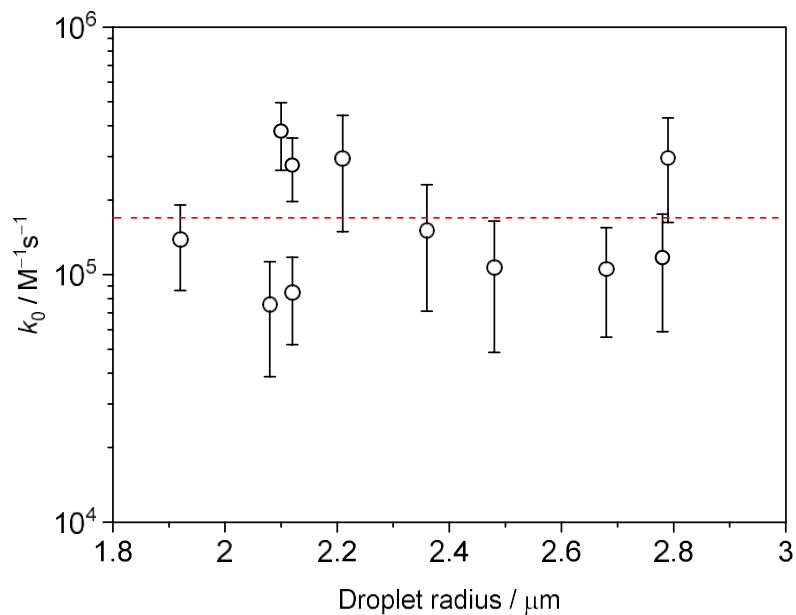


Figure S6. Bimolecular reaction rate coefficient corrected to zero ionic strength k_0 (symbols) of $\text{pH} \approx 2$ plotted as a function of droplet radius. Dashed line: the fitted value of k_0 obtained from the fit in Figure 4.

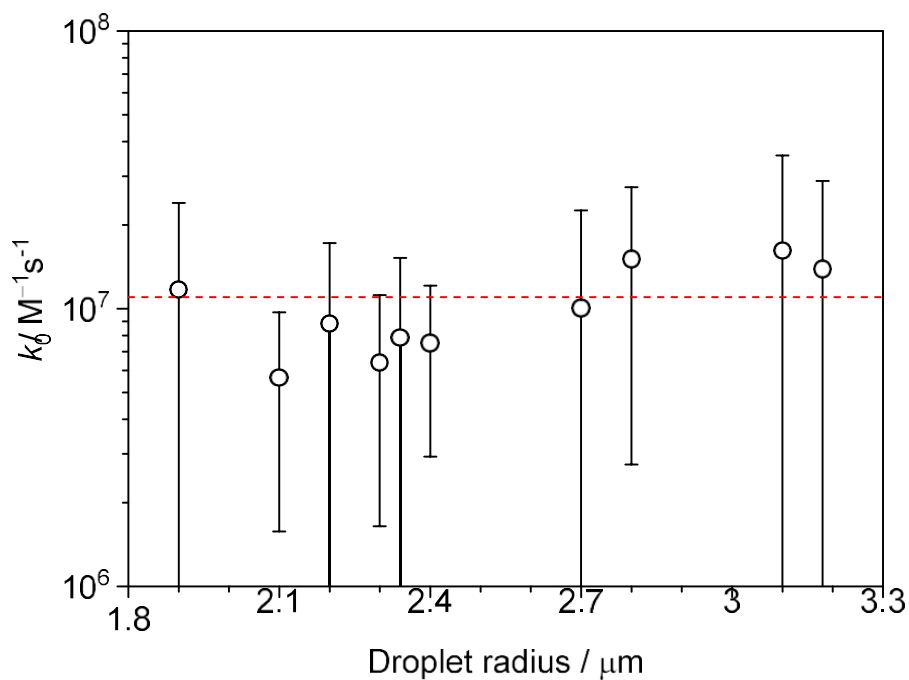


Figure S7. Bimolecular reaction rate coefficient corrected to zero ionic strength k_0 (symbols) of $\text{pH} \approx 6$ plotted as a function of droplet radius. Dashed line: the

fitted value of k_0 obtained from the fit in Figure 5.

References

- ¹R.W. Berg, *Appl. Spectrosc. Rev.* **50**, 193 (2015).
- ²S. Weisenberger and A. Schumpe, *AIChE J.* **42**, 298 (1996).
- ³A.K. Biń, *Ozone Sci. Eng.* **28**, 67 (2006).
- ⁴E. Rischbieter, A. Schumpe, and V. Wunder, *J. Chem. Eng. Data* **41**, 809 (1996).
- ⁵J.P. Burrows, A. Richter, A. Dehn, B. Deters, S. Himmelmann, S. Voigt, and J. Orphal, *J. Quant. Spectrosc. Radiat. Transf.* **61**, 509 (1999).